

## Immunoinformatics aided-design of novel multi-epitope based peptide vaccine against *Hendra henipavirus* through proteome exploration

Mohammad Imran Hossan<sup>a</sup>, Afrin Sultana Chowdhury<sup>a,\*</sup>, Mohammad Uzzal Hossain<sup>b</sup>, Md Arif Khan<sup>c</sup>, Tousif Bin Mahmood<sup>a</sup>, Shagufta Mizan<sup>d</sup>

<sup>a</sup> Department of Biotechnology and Genetic Engineering, Noakhali Science and Technology University, Noakhali, 3814, Bangladesh

<sup>b</sup> Bioinformatics Division, National Institute of Biotechnology, Dhaka, 1349, Bangladesh

<sup>c</sup> Department of Biotechnology and Genetic Engineering, University of Development Alternative, Dhaka, 1209, Bangladesh

<sup>d</sup> Department of Genetic Engineering and Biotechnology, University of Chittagong, Chittagong, 4331, Bangladesh



### ARTICLE INFO

#### Keywords:

*Hendra henipavirus*  
Multi-epitope vaccine  
Immunoinformatics  
Dynamics simulation

### ABSTRACT

*Hendra henipavirus* (HeV) is an emerging zoonotic bat-borne paramyxovirus that is capable of causing severe public health complications in humans. It promotes both respiratory and neurological disorders in humans as well as in horses. Currently, there are no therapeutics or vaccines available against the deadly HeV. We aimed to design a potent and novel prophylactic chimeric vaccine against HeV through an immunoinformatics approach. A proteome-wide screening was performed to identify the antigenic proteins followed by cytotoxic T-lymphocyte (CTL), linear B-lymphocyte (LBL), and helper T-lymphocyte (HTL) epitopes identification, conservancy analysis, population coverage, molecular docking and in silico simulation of both cellular and humoral immune response. A total of 17 T and B-cell epitopes (7 CTL, 5 HTL, and 5 LBL) were identified for vaccine design from the highest antigenic proteins, namely glycoprotein, fusion protein, and nucleoprotein. The proposed vaccine was found to be highly immunogenic, antigenic, non-toxic, non-allergenic, and stable, and could be efficient against HeV. Moreover, disulfide engineering and codon adaptation were employed to escalate stability and efficient expression in *E. coli*. Molecular docking and dynamics simulation analysis revealed the stability and strong affinity of the proposed vaccine towards the TL4 receptor. The immune simulation data confirmed elevated response of both B and T-cells against the vaccine subunit. The designed vaccine according to our in silico data is potent enough to elucidate substantial immune response and therefore can be considered as a potential immunogenic agent to control HeV infection. However, further experimental validation and clinical trials are required to confirm its efficacy and safety.

### 1. Introduction

*Hendra henipavirus* (HeV), a member of the henipavirus genus belonging to the paramyxovirus family caused several outbreaks in tropical regions of Australia in the last few years [1]. In September 1994, a previously unknown virus became responsible for an epidemic of severe respiratory illness in the Brisbane suburb of Hendra while thirteen horses died and two people got infected. It was the first official case of lethal zoonotic viral respiratory infection. This deadly virus was at first named *Equine morbillivirus* (EMV) and then named Hendra virus following the suburb origin from where it emerged [2–4]. HeV can cause fatal diseases in a broad range of mammalian hosts [5]; e.g. humans and horses by imposing severe respiratory and neurological infections [6].

HeV outbreak has been reported in each year since its first emergence and the frequency of occurrence of the HeV outbreak has remarkably increased from 2006 to 2010, with two incidents reported in every year except a single incident in 2010 [3,7]. As of June 2019, a total of 84 horses have died due to HeV infection [8].

The natural host of HeV is *Pteropus* spp. fruit bats. However, some recent studies claimed that the viral particle was transmitted to humans when they were exposed to infected horses [1–5,7]. The estimated incubation period of HeV is 7–10 days. Thereafter, the disease progression starts as an influenza-like illness, with nausea, vomiting, fever, headaches, lethargy, muscle pain. These symptoms varied between patients. In later stages of viral infection, the disease progresses by fulminating encephalitis that results in multi-organ failure. Oral-nasal routes appear

\* Corresponding author.

E-mail address: [afrin.bge@nstu.edu.bd](mailto:afrin.bge@nstu.edu.bd) (A.S. Chowdhury).

to be the main route of this viral infection, and the primary site of viral replication is the oral-nasal epithelium and upper respiratory tract [4]. The fatality rate of HeV infection in case of horse and human is 70% and 57%, respectively [1,2,7].

HeV are large enveloped, pleomorphic, and their size ranges from 40 to 600 nm in diameter. HeV genome is 18,234 nt long, non-segmented, single-stranded RNA with negative polarity, containing six transcriptional units namely Matrix protein gene (M), Fusion protein gene (F), Glycoprotein gene (G), Large polymerase protein gene (L), Nucleoprotein gene (N), and Phosphoprotein gene (P) which encode nine different proteins [1,2,4]. The RNA is tightly attached to the N protein and forms a complex with the P and L protein. The attachment of the virus with the host cell surface aided by G protein through a highly conserved mammalian protein, Ephrin B2 (EFNB2). The fusion of host cell membrane and viral cell membrane occurs with the help of F protein which facilitates virion release into the host cell [1]. The P gene products Phosphoprotein, non-structural protein W, non-structural protein V, and

non-structural protein C can modify the immune response by inhibiting the interferon activity [4].

Ever since HeV was identified as a newly emerged virus it has become a recurring threat to human and animal health. Genetic diversification, opportunistic nature, high virulence, extreme fatality rate, the capability to infect a broad range of mammalian hosts makes it one of the most devastating viruses that cause severe clinical complications to human health. However, the treatment option for HeV infection is still very limited. According to the report, the effect of Ribavirin in HeV infected golden hamster model was not significant. Also, an antimalarial drug Chloroquine when administered either individually or in combination with Ribavirin failed to show significant therapeutic outcome in hamsters infected with HeV [8,9]. Though there is one registered vaccine (Equivac® HeV) available to prevent HeV disease in horses [8], no licensed antiviral therapy or vaccine is available for humans. Given the severity of clinical manifestations of this virus among humans, development of a vaccine that can help prevent future HeV infections is in

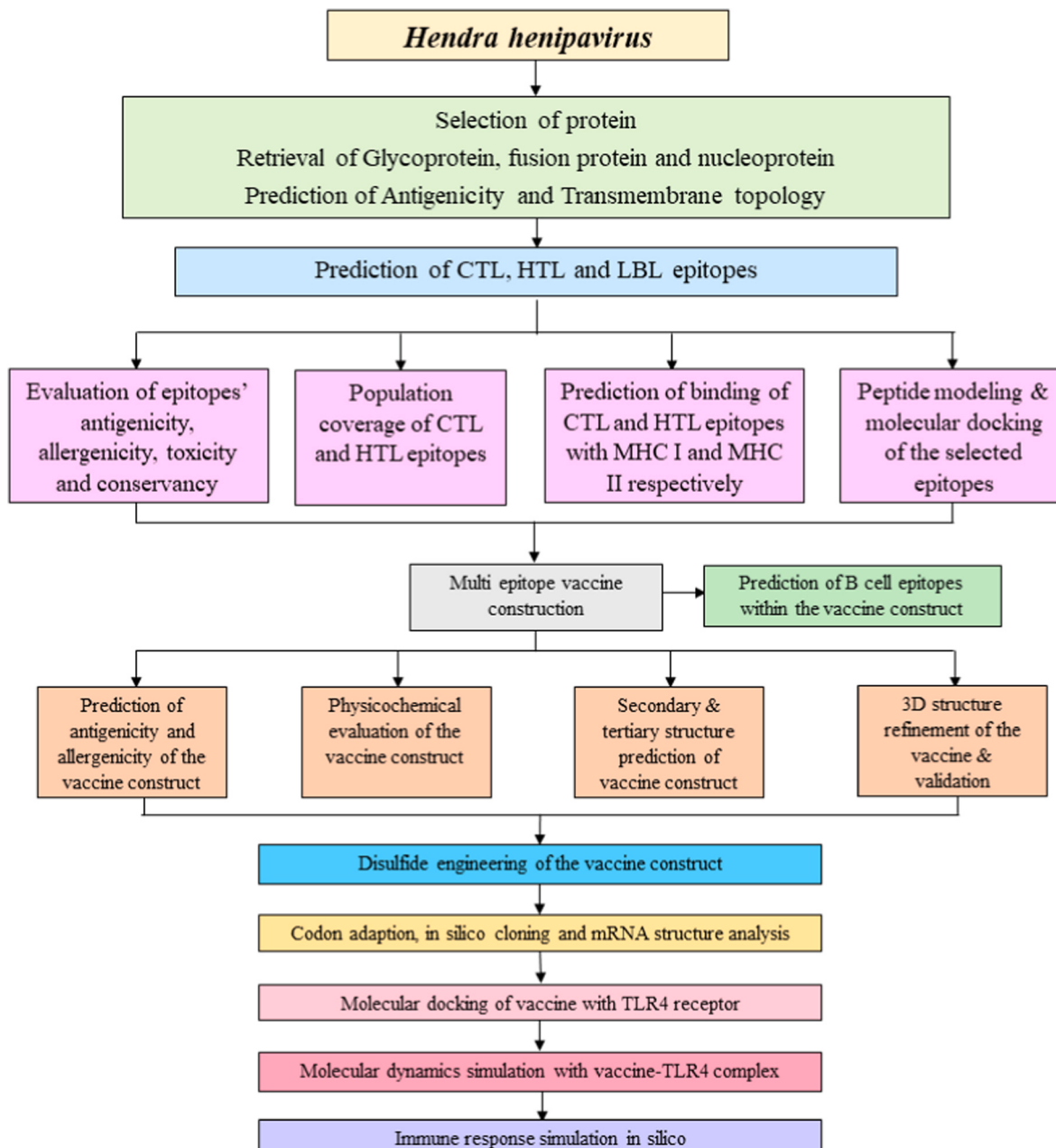


**Fig. 1.** Schematic representation of overall workflow used to design vaccine against *Hendra henipavirus*.

order.

Due to the recurring threat of HeV to public health and the absence of a suitable medication strategy, we aimed to design a prophylactic chimeric vaccine to prompt the immune reaction against HeV. Designing multi-epitope based vaccines through an *in silico* approach has become the gold standard for vaccine development in the post-genomic era because of its specificity and cost-effectiveness [10]. Therefore, we virtually screened the proteome of HeV to find out the most antigenic proteins followed by the multiple T (Cytotoxic T-lymphocyte and Helper T-lymphocyte) and B cell (Linear B-lymphocyte) epitopes prediction from selected antigenic proteins.

## 2. Materials and methods

The complete methodology of this study is represented in Fig. 1.

### 2.1. Protein sequences retrieval

The whole proteome of the HeV was scrutinized and then the FASTA sequences of all its proteins were retrieved from the UniProtKB (<http://www.uniprot.org/help/uniprotkb>) database using the following accession numbers O89343 (G protein), O89342 (F protein), O89341 (M protein), O89339 (N protein), o55778 (P protein), O89344 (RNA directed RNA polymerase), O55777 (non-structural protein V), O55779 (non-structural protein C), P0C1C6 (non-structural protein W). These proteins were further analyzed to look for their importance in the viral life cycle.

### 2.2. Identification of the highest antigenic proteins

VaxiJen 2.0 (<http://www.ddg-pharmfac.net/vaxijen/VaxiJen/VaxiJen.html>) was employed with a 0.5 threshold for all the essential proteins to calculate the antigenicity for plausible vaccine candidates [11]. This server is focused on auto cross-covariance (ACC) transformation and the alignment-independent prediction that maintains predictive accuracy of 70–89% [10]. Proteins that showed antigenicity above the threshold value were selected for further analysis [11].

### 2.3. Transmembrane topology prediction

TMHMM 2.0 (<http://www.cbs.dtu.dk/services/TMHMM/>) server focused on the hidden Markov model was utilized to find out the outer, inner, and transmembrane helical region of the selected proteins [12].

### 2.4. Identification and assessment of CTL epitopes

NetCTL 1.2 (<http://www.cbs.dtu.dk/services/NetCTL/>) tool was employed with a 1.25 threshold value to predict 9 amino acid length CTL epitopes from the previously selected protein sequences [13]. This server combines Human Leukocyte antigen (HLA) class -I binding, C-terminal cleavage, and TAP transport efficiency prediction algorithms to predict CTL epitopes for 12 (A1, A2, A3, A24, A26, B7, B8, B27, B39, B44, B58, B62) HLA super types [13]. In order to assess the antigenicity and immunogenicity of each of the predicted epitopes, VaxiJen server 2.0 [11] and IEDB class I immunogenicity (<http://tools.iedb.org/immunogenicity/>) tool [14] were utilized respectively. Two more Online tools - AllerTOP 2.0 (<https://www.ddg-pharmfac.net/AllerTOP/>) [15] and ToxinPred (<http://crdd.osdd.net/raghava/toxinpred/>) [16] were utilized to evaluate the allergenicity and toxicity of all the selected epitopes to be ensured of its safety. AllerTop 2.0 predicts allergenicity with 88.7% accuracy by combining auto cross-covariance (ACC) transformation and  $\kappa$ -nearest neighbor algorithm [15] while ToxinPred was set to SVM method to predict toxic CTL epitopes. To predict HLA class I binding alleles for initially selected CTL epitopes based on antigenicity, immunogenicity, toxicity, and allergenicity, the IEDB HLA class I tool (<http://tools.immuneepitope.org/mhci/>) [17] was used with IEDB

recommended 2020.04 method (NetMHCpan EL 4.0). In this study, the HLA source species parameter was set to human and the threshold value was considered 0.05 using the HLA reference set.

### 2.5. Identification and assessment of the HTL epitopes

IEDB MHC-II binding (<http://tools.iedb.org/mhcii/>) tool was utilized to predict the HTL epitopes of 15 amino acid length and their corresponding HLA class II alleles for multi-epitope based vaccine with the IEDB recommended method 22.2 [18]. This tool generates a percentile rank by comparing a set of random peptides from the SWISS-PROT database and the submitted peptides [18]. Therefore, percentile rank  $\leq 2$  was considered as the threshold value in our present study because a lower percentile rank implies greater binding affinity. From these predicted epitopes interferon-gamma (IFN- $\gamma$ ) producing HTL epitopes were filtered out by IFNepitope (<http://crdd.osdd.net/raghava/ifnepitope/>) tool [19] with the IFN- $\gamma$  versus Non-IFN- $\gamma$  model and hybrid method (Motif and SVM) parameters. Two more online tools- IL4pred (<http://crdd.osdd.net/raghava/il4pred/>) [20] and IL10pred (<http://crdd.osdd.net/raghava/il10pred/predict.php>) [21] was employed to evaluate interleukin- 4 (IL-4) and interleukin- 10 (IL-10) producing properties of predicted HTL epitopes with hybrid and SVM method respectively keeping other default parameters. Furthermore, AllerTOP 2.0 (<https://www.ddg-pharmfac.net/AllerTOP/>) [15] and ToxinPred (<http://crdd.osdd.net/raghava/toxinpred/>) [16] software were utilized to evaluate the allergenicity and toxicity of all the selected epitopes to be ensured of its safety.

### 2.6. Identification and assessment of the LBL epitopes

For linear B-lymphocyte (LBL) epitope prediction of varying lengths from protein sequence, two IEDB tools (<http://tools.iedb.org/bcell/>), namely Emini surface accessibility tool [22] and BepiPred linear epitope prediction 2.0 [23] were used. Epitopes predicted by both of the tools were selected for further analysis by submitting to the VaxiJen 2.0 tool [11] with a threshold value of 0.5.

### 2.7. Epitope conservancy analysis

The IEDB epitope conservancy analysis tool (<http://tools.iedb.org/conservancy/>) [24] was used to calculate the conservancy of the elected CTL, LBL, and HTL epitopes at the identity level of 100%.

### 2.8. Population coverage analysis

The IEDB population coverage (<http://tools.iedb.org/population/>) tool [25] was used to calculate the total percentage of people in a specific geographical region likely to give a response immunologically to the finally selected CTL and HTL epitopes and their respective HLA class I and II alleles tabulated in Tables 3 and 4.

### 2.9. Peptide modeling and molecular docking simulation studies

An online tool PEP-FOLD 3.0 (<https://mobyle.rpbs.univ-paris-diderot.fr/cgi-bin/portal.py#forms:PEP-FOLD3>) was utilized to model the selected CTL epitopes using 200 simulations with sOPEP sorting scheme. This tool predicts small peptides (5–50 amino acids) conformations using the Forward Backtrack/Taboo Sampling algorithm [26]. From the RCSB Protein Data Bank (<https://www.rcsb.org/search>) [27], the complex crystal structure (protein and epitope) of most conserved allele HLA-A\*24:02 (PDB ID: 2BCK) to be used as a receptor was retrieved in PDB format. Discovery studio was used to simplify the complex structure of HLA-A\*24:02 for the ease of docking study and then molecular docking was carried out using Autodock tools [28] and AutodockVina software [29]. The grid box center was set at 35.376, 17.076, and 3.458 Å in the X, Y, and Z-axis, respectively, and the

grid size was set at 76, 60, and 86 Å in the X, Y, and Z dimensions, respectively to get the binding energy of HLA-A\*24:02 with an epitope at the HLA groove. Finally, the docking simulation study was performed at a 0.681 Å spacing parameter using the AutoDockVina tool. To make and visualize the docked receptor-epitope complex, the PyMOL [30] molecular graphics system and Discovery studio 2017 were used respectively. The experimentally validated crystal structure of two common HLA class II alleles (HLA-DRB3\*02:02 and HLA-DRB\*15:02) for predicted HTL epitopes were not found in RCSB Protein Bank, hence docking of HTL epitopes was not performed.

#### 2.10. Construction of multi-epitope vaccine

The expression of TLR4 increases during infection and TLR4 agonists are frequently used as a part of the peptide-based subunit vaccine [31]. Adjuvants play an important role to boost the immune response against an antigen and initiate a specific, long-lasting immune response with the help of various immune mechanisms [32]. For this reason, 50S ribosomal protein L7/L12, a Toll-like receptor 4 (TLR4) agonist was retrieved from the UniProtKB database (Accession no. P9WHE3) to be used as an adjuvant at N-terminal of the sequence. Another protein namely human beta-defensin 2 (Accession No. 1FD3) was retrieved from RCSB protein data bank and added to the C-terminal of the vaccine sequence. Two peptide linkers namely, GPGPG, and AAY were used to separate the epitopes and ensure the individual immune responses within the human body. The GPGPG linker was used to join the two adjuvant 50S ribosomal protein L7/L12 and human beta-defensin at N and C-terminal of vaccine sequence respectively [34].

#### 2.11. Evaluation of the vaccine construct

VaxiJen 2.0 [11] and ANTIGENpro (<http://scratch.proteomics.ics.uci.edu>) [35] tools were utilized to assess the antigenicity of the constructed vaccine. The immunogenicity and allergenicity were evaluated by the IEDB Immunogenicity tool [14] and AllerTOP 2.0 [15].

The physicochemical features of the constructed vaccine, i.e., molecular weight (MW), aliphatic index (AI), theoretical isoelectric point (PI), instability index (II), grand average of hydropathicity (GRAVY), and in vitro and in vivo half-life were evaluated using the ProtParam tool (<https://web.expasy.org/protparam/>) of the Expasy server [36]. Furthermore, the SOLpro tool (<http://scratch.proteomics.ics.uci.edu>) [37] was used to predict the propensity of vaccine protein to be soluble upon overexpression in *E. coli* was predicted and confirmed by Protein-Sol (<https://protein-sol.manchester.ac.uk/>) tool [38].

#### 2.12. Prediction of the vaccine's secondary and tertiary structure

PSIPRED v4.0 (<http://bioinf.cs.ucl.ac.uk/psipred/>) [39] was used to predict the vaccine's secondary structure, which is a highly accurate secondary structure prediction tool from the amino acid sequence by combining feed-forward neural networks and PSIBLAST (Position-Specific Iterated-Blast) [39]. Next, we used the Iterative Threading Assembly Refinement (I-TASSER) tool (<https://zhanglab.ccmb.med.umich.edu/I-TASSER/>) [40] to predict the 3D structure of our final vaccine construct. This tool generates homology models by iterative template-based fragment assembly simulations [40]. Pymol was used to visualize the best 3D model from I-TASSER output.

#### 2.13. Refinement and validation of the vaccine's 3D structure

The generated raw model of vaccine protein was first refined by the 3Drefine tool (<http://sysbio.rnet.missouri.edu/3Drefine/>) [41], which refines the structure by minimizing atomic-level energy and optimizing hydrogen bonding network. After that, GalaxyRefine (<http://galaxy.seoklab.org/refine>) [42] was used to refine the structure by structural relaxation through molecular dynamics simulation to improve the

average global and local structure quality. Therefore, the refined structure was submitted to ProSA-web (<https://prosa.services.came.sbg.ac.at/prosa.php>) [43] for structural validation by calculating an overall quality score. The difference between the range of native and predicted quality score is the indication of possible errors in the predicted tertiary structure. Furthermore, the Swiss model interactive workspace (<https://swissmodel.expasy.org/assess>) [44] of the Expasy server is employed for structural validation and to generate a Ramachandran plot.

#### 2.14. Prediction of B-cell epitopes in the vaccine construct

To confirm the presence of both linear and conformational B-cell epitopes in the vaccine construct, the ElliPro tool of the IEDB server (<http://tools.iedb.org/ellipro/>) [45] was utilized with default parameters.

#### 2.15. Disulphide engineering of the final vaccine construct

The refined vaccine structure was submitted to the Disulphide by Design (DbD) 2.12 (<http://cptweb.cpt.wayne.edu/DbD2/>) [46] tool to increase stability by creating disulphide bond between potential residue pair. Based on a set of criteria, potential residue pairs were selected and mutated with a cysteine residue [46].

#### 2.16. Codon optimization, in silico cloning, and mRNA structure prediction

To ensure efficient expression of the vaccine protein in *E. coli* K12, codon adaptation was carried out using Java Codon Adaptation Tool (JCAT) (<http://www.jcat.de/>) [47]. Three parameters were checked to avoid the restriction enzyme cleavage sites, rho-independent transcription termination, and prokaryotic ribosome binding site during the codon adaptation process. Furthermore, EcoRI and BamHI restriction sites were introduced to the N and C-terminal of the vaccine sequence, respectively. Finally, cloning simulation between the adapted nucleotide sequence corresponding to the designed vaccine construct and the *E. coli* pET28a(+) expression vector was carried out by using the SnapGene 4.2 software (<https://www.snapgene.com/>).

RNAfold (<http://rna.tbi.univie.ac.at/cgi-bin/RNAWebSuite/RFold.cgi>) online tool was utilized to generate the mRNA secondary structure which predicts the mRNA structures thermodynamically and assigns a minimal free energy score [48–50]. The optimized DNA sequence generated by the JCat tool were then converted to RNA sequence by DNA>RNA>Protein tool (<http://biomodel.uah.es/en/lab/cybertory/analysis/trans.htm>) and submitted to the RNA fold server keeping default parameters.

#### 2.17. Molecular docking between the vaccine and TLR4 receptor

To check the binding affinity between TLR4 (as a receptor, PDB ID: 4G8A) and designed multi-epitope vaccine (as a ligand), a molecular docking study was done with the help of ClusPro 2.0 server (<http://cluspro.bu.edu/>) [51]. ClusPro is a top-notch tool for protein-protein docking and generates binding affinity by combining three successive steps: rigid-body docking, clustering of lowest energy structure, and structural refinement by energy minimization [51].

#### 2.18. Molecular dynamic simulation studies for vaccine stability

Molecular dynamics simulation by the i-MODS tool (<http://imods.chaconlab.org>) [52] was done to assess the stability of the receptor-vaccine complex in the biological environment. This tool estimates the protein-protein complex dynamics by calculating the deformability, B-factors, eigenvalues, covariance, and elastic network [52].

## 2.19. In silico immune response simulation

C-ImmSim (<http://www.cbs.dtu.dk/services/C-ImmSim-10.1/>) tool was employed to evaluate the real-life immunogenic profile of the engineered chimeric vaccine [53]. It is an antigen-based immune simulator that predicts immune reactions by combining a machine learning algorithm and position-specific scoring matrix (PSSM) [53]. The standard rule in practice for most vaccines is that the minimum time interval between the two doses should be four weeks [54]. A total of three injections of 1000 antigens each were administered at 8 weeks and 24 weeks interval after first shot at 1, 168 and 504 time-steps (each time step is equal to 8 h in real-life and time-step 1 is injection at time = 0). The simulation steps parameter was set to 1050 while keeping others parameters default. The measure of diversity, D (Simpson's Diversity Index) was interpreted from the generated figures.

## 3. Results

### 3.1. Highest antigenic proteins prediction

To induce both cell-mediated and humoral immunity, highly antigenic proteins of the virus must be selected [55]. VaxiJen 2.0 tool was employed to assess the antigenicity of HeV proteins, which renders antigenicity by assigning a score; a higher score above the threshold value (0.5) indicates greater antigenicity. As per our findings, the G protein, F protein, and N protein had the highest antigenicity compared to the other HeV proteins (Table 1). Therefore, those proteins were selected to induce both cell-mediated and humoral immunity efficiently and analyzed further.

### 3.2. Transmembrane topology of the selected proteins

In vaccine design, it is necessary for the selected epitopes to be in the exposed region of the protein to provoke an efficient immune response. The transmembrane topology analysis of the G, F and N proteins was done by using TMHMM and the result revealed that the length of exo-membrane amino acid sequences for glycoprotein, fusion protein, and nucleoprotein were 70–602, 30–495, and 1–532 respectively (Table 2).

### 3.3. Identification and assessment of CTL epitopes

T-cell epitopes are mostly small peptides having the capacity of inducing an immune response and specific antigen recognition occurs through a specific T-cell receptor (TCRs) expressed by cytotoxic T-cell [56]. In this study, we found 198, 238, and 177 nonamer unique CTL epitopes for G protein, F protein, and N protein respectively by NetCTL 1.2 tool. Epitopes should be non-toxic and non-allergenic because toxic and allergenic epitopes can compromise the aim of vaccine development. So, predicted epitopes were subjected to antigenicity, immunogenicity evaluation (Supplementary Tables 1, 2, 3). Among them, epitopes having both positive immunogenicity and antigenicity ( $\geq 0.5$ ) were selected for further allergenicity and toxicity prediction by the AllerTop and ToxinPred tools respectively (Supplementary Tables 4, 5,

**Table 1**  
Predicted antigenicity of the HeV proteins.

Protein	Predicted antigenicity
Nucleoprotein	0.5308
Phosphoprotein	0.4676
Non-structural protein V	0.4864
Non-structural protein W	0.4667
Non-structural protein C	0.3450
Matrix protein	0.4332
Fusion protein	0.5529
Glycoprotein	0.5367
Polymerase protein	0.4806

**Table 2**

Transmembrane topology of the Glycoprotein, Fusion protein and Nucleoprotein.

Name of the protein	Position	Amino acid
<b>Glycoprotein</b>	Inside	1–46
	TMHelix	47–69
	Outside	70–602
<b>Fusion protein</b>	Inside	1–6
	TMHelix	7–29
	Outside	30–495
<b>Nucleoprotein</b>	TMHelix	496–518
	Inside	519–546
	Outside	1–532

6). After this, 17, 20, and 17 epitopes of G protein, F protein, and N protein respectively were found as immunogenic, antigenic, non-toxic, and non-allergenic. The HLA class I molecule binds and puts forward the peptides to CD8<sup>+</sup> which can induce cellular immunity against a foreign antigen. So, these epitopes were further subjected to corresponding HLA class I binding alleles prediction by the HLA class I allele prediction tool of the IEDEB server (Supplementary Tables 7, 8, 9).

### 3.4. Identification and assessment of HTL epitopes

Helper T-cells are the key mediator of the immune response of the adaptive immune system and the HLA class II molecule binds and puts forward the peptides to CD4<sup>+</sup> cells that can induce humoral and cellular immunity against the pathogen [57]. A total of 55, 94 and 26 pentadecamer HTL epitopes and their corresponding HLA class II binding alleles were predicted for G protein, F protein, and N protein respectively using the IEDEB HLA class II binding tool. After that, predicted HTL epitopes were evaluated for their cytokine inducing (i.e., IFN- $\gamma$ , IL-4, and IL-10) ability by IFNepitope, IL4pred, and IL410pred tool respectively. (Supplementary Tables 10,11,12). Cytokines play a crucial role in initiation and determination of antiviral immune response and subsequent downstream effector mechanism. IFN- $\gamma$  induces T helper type 1 (Th-1) responses by variety of mechanisms such as induction of apoptosis, activation of APC, up-regulation of HLA class I and II molecules while IL-4 instigates T helper type 2 (Th-2) responses [58]. IL-10 being an anti-inflammatory cytokine, the effects of IL-10 depend on the site of infection, virus and timing of the antiviral response [59]. It can positively act to balance the pathogen specific immune response by stimulating various mechanisms contributing to the viral clearance, B cell proliferation and antibody formation [59]. In influenza infections, production of both IL-10 and IFN- $\gamma$  facilitates anti-influenza antibody accumulation in the lung mucosa [60]. Only 10, 6, and 4 HTL epitopes of G protein, F protein, and N protein respectively were found capable of inducing IFN- $\gamma$ , IL-4, and IL-10 cytokines (Supplementary Table 13). The cytokine-inducing HTL epitopes were further evaluated for antigenicity and toxicity by AllerTop and ToxinPred respectively (Table 4).

### 3.5. Identification and assessment of LBL epitopes

B-cell epitopes are mainly the antigenic region of a protein that can be recognized by the immunoglobulin molecules to induce B-cell response. B-cell epitopes play an important role in peptide-based vaccine design, and also in disease diagnosis [60]. The B-cell epitopes must be antigenic and surface accessible to elicit sufficient immune response. A total of 21, 20, and 16 epitopes of variable length were predicted by the BepiPred linear epitope prediction 2.0 tool for glycoprotein, fusion protein, and nucleoprotein respectively. On the other hand, 13, 11, and 9 epitopes were predicted by the Emini surface accessibility tool of IEDEB for glycoprotein, fusion protein, and nucleoprotein respectively (Supplementary Table 14, 15 and 16). Common epitopes predicted by both of the tools were then subjected to antigenicity evaluation by the Vaxijen (Supplementary Table 17).

**Table 3**

Finally, selected CTL epitopes from Glycoprotein, Fusion protein and Nucleoprotein.

Protein name	Epitope sequence	Position	Combined score	Antigenicity	Immunogenicity	Allergenicity	Toxicity	HLA class I binding alleles	Conservancy
Glycoprotein	FLPRTEFQY	369–377	0.9256	1.0880	0.21165	No	No	HLA-B*15:01, HLA-A*01:01, HLA-A*68:01, HLA-B*35:01, HLA-A*30:02 HLA-B*35:01, HLA-A*26:01, HLA-A*32:01, HLA-A*02:06 HLA-B*53:01, HLA-A*23:01, HLA-A*24:02, HLA-B*58:01,	100.00%
	ITIPANIGL	118–126	1.1357	1.1090	0.19617	No	No	HLA-A*02:06, HLA-B*58:01, HLA-A*68:02, HLA-B*57:01, HLA-A*32:01, HLA-A*02:01, HLA-A*02:03, HLA-A*30:01, HLA-A*26:01, HLA-A*23:01, HLA-A*68:02, HLA-B*15:01, HLA-B*51:01, HLA-A*30:02, HLA-A*68:01, HLA-A*24:02, HLA-B*53:01, HLA-B*35:01, HLA-A*01:01,	100.00%
	RIJGVGEVL	258–256	0.8749	0.7453	0.25802	No	No	HLA-A*32:01 (0.6498, 0.07) HLA-A*02:06 (0.4764, 0.34) HLA-A*02:03 (0.4193, 1.0) HLA-B*15:01 (0.4067, 0.39) HLA-B*58:01 (0.3085, 0.68) HLA-A*02:01 (0.2710, 0.83) HLA-A*02:03 (0.2015, 2.3) HLA-B*57:01 (0.1956, 0.82) HLA-B*07:02 (0.1941, 0.65) HLA-A*68:02 (0.1262, 1.5) HLA-A*30:01 (0.1147, 1.7) HLA-A*33:01 (0.0905, 2.0) HLA-A*30:02 (0.0673, 2.0) HLA-A*24:02 (0.0634, 2.4) HLA-B*35:01 (0.0509, 2.0) HLA-A*02:06 (0.0503, 3.7)	100.00%
Fusion protein	VMAGIAIGI	114–122	1.1844	1.1266	0.34535	No	No	HLA-A*02:03, HLA-A*02:01, HLA-A*02:06, HLA-A*32:01, HLA-B*51:01, HLA-A*68:02, HLA-A*23:01, HLA-A*24:02, HLA-B*58:01, HLA-B*15:01	100.00%
	ISIVPNFVL	309–317	1.5973	0.9248	0.19077	No	No	HLA-B*58:01, HLA-B*57:01, HLA-B*08:01, HLA-A*32:01, HLA-A*02:06, HLA-B*51:01, HLA-A*68:02, HLA-B*51:01, HLA-A*23:01, HLA-A*30:01	100.00%
Nucleoprotein	NMQAREAKF	407–415	1.1395	1.1858	0.05344	No	No	HLA-B*08:01, HLA-B*15:01, HLA-B*15:01, HLA-A*24:02, HLA-A*23:01, HLA-B*58:01	100.00%
	KFAPGGYPL	321–329	0.9561	1.0107	0.05684	No	No	HLA-A*24:02, HLA-A*23:01, HLA-A*32:01, HLA-B*51:01, HLA-A*30:01, HLA-A*30:02, HLA-A*31:01, HLA-A*02:06, HLA-B*08:01, HLA-B*15:01, HLA-B*07:02, HLA-A*02:03, HLA-B*58:01, HLA-A*02:01, HLA-B*35:01, HLA-B*08:01	100.00%

**Table 4**

Finally, selected HTL epitopes from Glycoprotein, Fusion protein and Nucleoprotein.

Protein	Epitope sequence	Position	HLA class II binding alleles	Antigenicity	IFN-Gamma Inducing	IL4 inducing	IL10 inducing	Allergenicity	Toxicity
Glycoprotein	PLRVQWRNNNSVISRP	474–488	HLA-DRB3*02:02	1.1398	Positive	Positive	Positive	No	No
	DPLRVQWRNNNSVISR	473–487	HLA-DRB3*02:02	1.2337	Positive	Positive	Positive	No	No
Fusion protein	CIGLITFISFVIVEK	506–520	HLA-DRB1*15:01	1.3166	Positive	Positive	Positive	No	No
	GLITFISFVIVEKKR	508–522	HLA-DRB1*15:01	1.5633	Positive	Positive	Positive	No	No
Nucleoprotein	KGKTPFVDSRAYGLR	140–154	HLA-DRB1*07:01	0.4467	Positive	Positive	Positive	No	No

### 3.6. Selection of CTL, HTL and LBL epitopes

Finally, 424 amino acids long multi-epitope vaccine was constructed by combining adjuvant (121 amino acid long 50S ribosomal protein L7/L12) and 17 T and B-cell epitopes (7 CTL, 5 HTL, and 5 LBL). Epitopes

were merged by specific linkers in appropriate position, for example, EAAAK linker was used to join adjuvant and first CTL epitope, namely <sup>369</sup>FLPRTEFQY<sup>377</sup>, <sup>118</sup>ITIPANIGL<sup>126</sup>, <sup>362</sup>LYFPAVGFL<sup>370</sup>, <sup>114</sup>VMA-GIAIGI<sup>122</sup>, <sup>309</sup>ISIVPNFVL<sup>317</sup>, <sup>407</sup>NMQAREAKF<sup>415</sup>, <sup>321</sup>KFAPGGYPL<sup>329</sup> were found to be recognized by the highest number of HLA class I alleles

and having highest immunogenicity and antigenicity value, non-toxic and non-allergenic were selected as the potential epitope for multi-epitope vaccine design (Table 3). We selected 100% conserved 5 highly antigenic HTL epitopes namely <sup>474</sup>PLRVQWRNNNSVISRP<sup>488</sup>, <sup>473</sup>DPLRVQWRNNNSVISR<sup>487</sup>, <sup>506</sup>CIGLITFISFVIVEK<sup>520</sup>, <sup>508</sup>GLITFISFVI-VEKKR<sup>522</sup>, <sup>140</sup>KGKTPFVDSRAYGLR<sup>154</sup> having the ability to induce all three kinds of cytokines (Table 4). Furthermore, 100% conserved 5 LBL epitopes with highest antigenic score <sup>165</sup>PLPFREYRPI174, <sup>372</sup>RTEF-QYNDS<sup>380</sup>, <sup>48</sup>IKNPL<sup>54</sup>, <sup>402</sup>GRQDNMMQAREA<sup>413</sup>, <sup>427</sup>QDIDEEEPI<sup>436</sup> were selected for vaccine design (Table 5).

### 3.7. Conservancy and population coverage analysis of the selected epitopes

Conservancy indicates a specific region of a protein sequence that represents the epitope and shows availability with a specific level of identity. The conservancy of most potential epitopes was assessed because, in vaccine design, epitopes must show a considerable amount of conservancy [61].

The expression of HLA class I and II alleles differ significantly in different ethnicities, so evaluation of HLA alleles distribution (population coverage) is an important criterion for rational vaccine design [61]. If epitopes bind to the HLA alleles with a frequency of 100% or near 100% in a specific population, then these epitopes are considered plausible epitopes for vaccine design. Finally, Individual and combinatorial population coverage for the selected 12 T-cell epitopes (7 CTL and 5 HTL) with their corresponding HLA alleles were reckoned as tabulated in Supplementary Table 18. Global population coverage of 92.8% and 34.78% were found for CTL and HTL epitopes, respectively. In this study, importance was given to the combined population coverage because both CTL and HTL epitopes were used to construct the vaccine. Results show that combined population coverage was found 95.3% and 99.9% individuals will respond to the selected epitopes in Peru. The population coverage for Australia where the virus first emerged was 85.05% (Fig. 2).

### 3.8. Molecular docking simulation studies between HLA-A\*24:02 and CTL epitopes

A molecular docking simulation study is the best way to check the interaction and calculate the binding affinity between receptor and ligand molecules. To get maximum population coverage, it is a prerequisite to select epitopes showing binding affinity to the highest number of alleles for vaccine designing. In this study, we selected experimentally validated HLA-A\*24:02 that has binding interaction with most of the selected epitopes. Molecular docking was performed between selected 7 CTL epitopes and HLA-A\*24:02. A total of 9 binding models were generated for each epitope and depending on the number of hydrogen bonds and binding energy top binding models were chosen. Best models with their binding energy, number of hydrogen bonds and interacting residues are shown in Fig. 3 and listed in Table 6.

### 3.9. Construction of multi-epitope vaccine construct

Finally, a 424 amino acids long multi-epitope vaccine was constructed by combining two adjuvants (130 amino acid long 50S

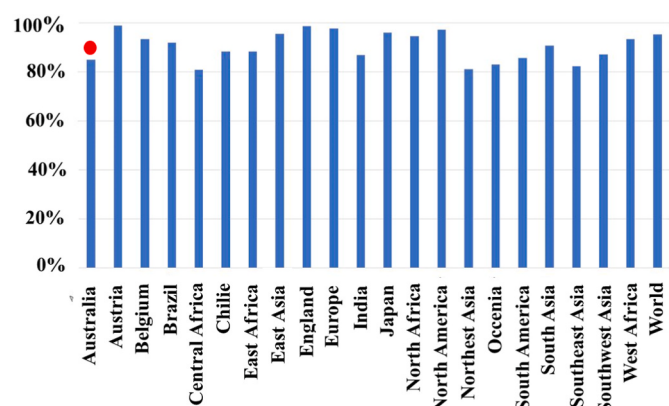


**Fig. 2.** Combined population coverage of selected CTL and HTL epitopes. X-axis indicates combined population coverage (HLA I and II) and Y-axis indicates name of the country. Red dot indicates the region where HeV was first emerged. (For interpretation of the references to color in this figure legend, the reader is referred to the Web version of this article.)

ribosomal protein L7/L12 and 41 amino acid long human beta-defensin) and 17 T and B-cell epitopes (7 CTL, 5 HTL, and 5 LBL). Epitopes were merged by specific linkers in appropriate position, for example, GPGPG linker was used to join the first adjuvant at N-terminal end of vaccine, intra-CTL, intra-HTL epitopes and intra-LBL epitopes were joined together by AAY and GPGPG linker. The arrangement of adjuvant and epitopes with their joining linkers is shown in Fig. 4.

### 3.10. Evaluation of the multi-epitope vaccine construct

To elicit sufficient immune response after administration without any side effects, it is a crucial prerequisite for vaccine constructs to be highly antigenic and immunogenic, non-toxic, and non-allergic [55]. The results labeled the vaccine construct as probable antigen and immunogen and non-allergen (Table 7).

The vaccine construct was predicted to be stable, basic, hydrophilic, thermostable, and highly soluble upon over-expression in *E.coli* based on the evaluation of physicochemical properties. Furthermore, the half-life of the vaccine in mammalian reticulocytes (in vitro) was found to be 30 h, in yeast (in vivo), and *E.coli* (in vivo) over 20 h and over 10 h respectively. The analysis result of physicochemical parameters is tabulated in Table 7.

### 3.11. Prediction of the secondary and tertiary structure of the vaccine construct

After analysis by PSIPRED, the result showed that in the vaccine construct, random coils are formed by 242 amino acids,  $\alpha$ -helix by 148 amino acids and  $\beta$ -strands are formed only by 34 amino acids. The overall secondary structure prediction results concluded that 57.07% are random coils, 34.90% form  $\alpha$ -helix and 8.01% are  $\beta$ -strands (Supplementary Fig. 1).

A total of 5 models were generated by I-TASSER for vaccine protein and based on the predicted C-score ( $-0.89$ ), model 1 was chosen. C-score refers to the quality of predicted models generally lies in the range

**Table 5**

Finally, selected LBL epitopes from Glycoprotein, Fusion protein and Nucleoprotein.

Protein name	Epitope sequence	Position	Length	Antigenicity	Conservancy
<b>Glycoprotein</b>	PLPFREYRPI	165–174	10	1.3026	100%
	RTEFQYNDS	372–380	9	1.1542	100%
<b>Fusion protein</b>	IKNPL	48–53	6	1.3014	100%
	GRQDNMMQAREA	402–413	12	1.086	100%
<b>Nucleoprotein</b>	QDIDEEEPI	427–436	10	0.5533	100%

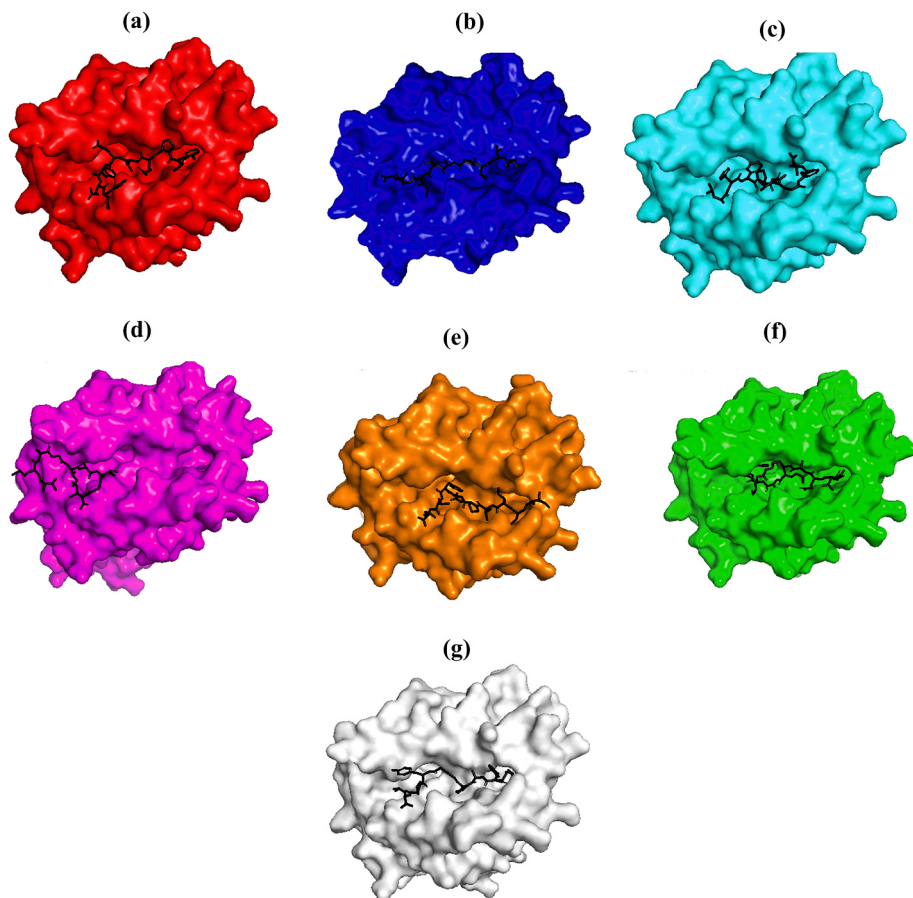


**Fig. 3.** Molecular docking simulation study showing HLA-A\*24:02 as surface and CTL epitopes as sticky form. 1. HLA-A\*24:02 and FLPRTTEFQY 2. HLA-A\*24:02 and ITIPANIGL 3. HLA-A\*24:02 and LYFPAVGFL 4. HLA-A\*24:02 and VMAGIAIGI 5. HLA-A\*24:02 and ISIVPNFVL 6. HLA-A\*24:02 and KFAPGGYPL 7. HLA-A\*24:02 and NMQAREAKF.

**Table 6**  
Molecular docking simulation results of CTL epitopes with HLA-A\*24:02.

Serial No.	HLA Class I binding peptide	Docking score (kcal/mol)	Number of Hydrogen bond	Interacting residues (One letter code)
01	FLPRTTEFQY	-7.4	10	N77, W147, Q155, Q156, T163, F1, Q8, T163, K66, H114, Y123, Y159, Y116, K146, R4
02	ITIPANIGL	-7.1	07	K66, T73, W147, R170, T143, N77, T2, I80, V152, H70
03	LYFPAVGFL	-7.7	02	K146, Q156, P4, L9, T143, V6, F99, H70, W147, W159, Y2, F8
04	VMAGIAIGI	-5.6	06	Y59, K66, T163, G8, I9, R170, V1, Y159
05	ISIVPNFVL	-6.0	04	K146, W147, Q155, T163, V8, M97, H70, I80, A150
06	KFAPGGYPL	-7.1	08	T73, N77, Y116, Q156, Y159, F9, Q3, F9, V67, A7, M2, Y7, F99, K66, A69, I80, H114, Y159
07	NMQAREAKF	-7.5	04	Y84, T143, Q155, T163, K1, K66, A81, V152, Y123, Y7

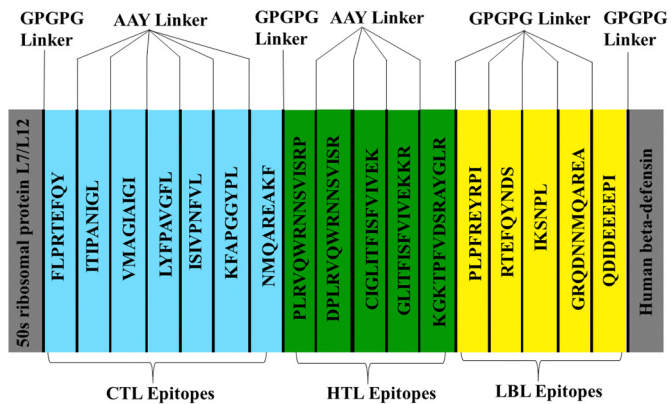


**Fig. 4.** Structural arrangement of final vaccine candidate constructed from adjuvant, CTL, HTL and LBL epitopes separated by linkers.

of [-5,2] where a higher score signifies higher model quality. Fig. 5 represents the tertiary structure of the vaccine protein.

### 3.12. Refinement and validation of the tertiary structure

The 3Drefine online tool was used to carry out the first phase of refinement of the predicted tertiary structure. Out of the 5 models generated by 3Drefine, based on the 3Drefine Score (35702.3), GDT-TS (1.0000), GDT-HA (0.9982), RMSD (0.192), MolProbity (3.335), and RWPlus (-67535.629149) model 1 was selected to refine further. In

**Table 7**  
Physiochemical evaluation of vaccine construct.

Parameter	Result
Chemical formula	C <sub>2043</sub> H <sub>3198</sub> N <sub>534</sub> O <sub>580</sub> S <sub>12</sub>
Molecular weight	44905.82
Number of amino acids	424
Theoretical PI	8.49
Aliphatic Index	85.73
Instability Index	30.91
Grand average of hydropathicity (GRAVY)	-0.004
Estimated half-life ( <i>Escherichia coli</i> , in vivo)	>10 h
Estimated half-life (mammalian reticulocytes, in vitro)	30 h
Estimated half-life (yeast cells, in vivo)	>20 h
Extinction coefficient (at 280 nm in H <sub>2</sub> O)	38,195 M <sup>-1</sup> cm <sup>-1</sup>
Immunogenicity	4.86
Antigenicity	0.72 (Vaxijen) 0.83 (ANTIGENpro)
Allergenicity	No
Solubility	0.78 (SOLpro) 0.46 (Protein-Sol)

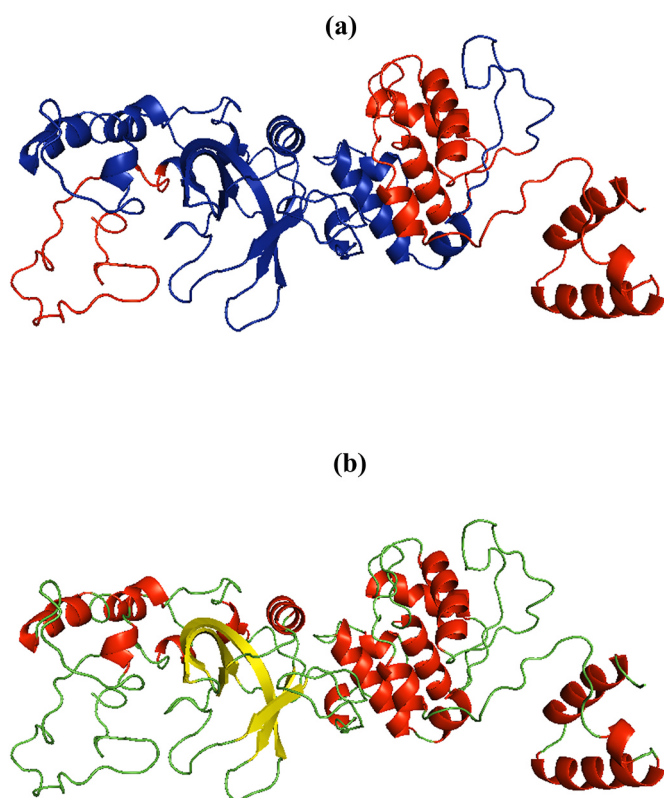


**Fig. 5.** Tertiary structure of the vaccine construct. (a) Red color represents the adjuvant and blue color represents vaccine. (b) Red, yellow and green indicates helix, sheet and random coil respectively. (For interpretation of the references to color in this figure legend, the reader is referred to the Web version of this article.)

order to increase the overall quality of the model, GalaxyRefine tool was used for the second phase of refinement. From the results obtained model 1 proved to be best based on RMSD (0.312), MolProbity (2.178), Clash score (16.8), Rama favored (92.9%), GDT-HA (0.9764), Poor rotamers (0.6%). Therefore, evaluating various parameters, this model was taken as the final vaccine model. The refinement results by 3Drefine and GalaxyRefine are tabulated by [Supplementary Tables 19 and 20](#).

Structural validation process based on comparing the experimentally validated model and predicted model is the best way to check the correctness of the predicted tertiary structure in homology modeling. Swiss model interactive workspace structure assessment showed that

Qualitative model energy analysis (QMEAN) score was -2.36 and from Ramachandran plot, we found that 315 (92.9%) amino acid lies in the Rama-favored region, 20 (5.8%) amino acid in the allowed region and only 3 (0.8%) amino acid in the disallowed region ([Supplementary Fig. 2a](#)). Moreover, ProSA-web calculated the Z-score of -3.44 which lies within the range of experimentally proven native X-ray crystal structures of comparable size from the Protein Data Bank ([Supplementary Fig. 2b](#)).

### 3.13. Mapping of B-cell epitopes in the vaccine protein

B-lymphocyte enhances humoral immunity by secreting antibodies and cytokines to neutralize foreign antigen [62] which is why it is important to have sufficient B-cell epitopes within the protein domain. The presence of linear and conformational B-cell epitopes was assessed using the ElliPro tool of the IEBD server and identified a total of 12 linear B-cell epitopes of 4–49 residues with scores ranging from 0.508 to 0.855 ([Fig. 6a](#)). A total of 9 conformational B-cell epitopes of 3–78 residues were identified with scores ranging from 0.528 to 0.855 ([Fig. 6b](#)).

### 3.14. Disulfide engineering for vaccine protein stability

A total of 36 potential residue pairs were identified after subjecting the vaccine sequence in the Disulfide by Design 2.12 tool that can form a disulfide bond as tabulated in [Supplementary Table 21](#). Keeping the bond energy and  $\chi_3$  parameters into consideration, only a residue pair was selected because their scores meet standard criteria i.e. the bond energy should be less than 2.2 kcal/mol and  $\chi_3$  angle should be in the range of -87 and + 97° [49]. A mutation pair was generated on the residue pair, A199-G323 which has a bond energy of 1.33 kcal/mol and  $\chi_3$  angle of +89.17° as shown in [Fig. 7](#).

### 3.15. Codon adaptation, in silico cloning and mRNA structure analysis

The difference in codon usage results in the low translation of foreign genes and for this reason codon adaptation is the best way to increase translational efficiency [56]. JCat tool was used to optimize the codon usage of our designed vaccine with respect to the *E.coli* K12 strain. Results showed that the GC content of the optimized sequence was 53.06% which indicates the efficient expression in the *E.coli* host with a Codon adaptation index (CAI) of 0.96. After that, the adapted codon sequence of vaccine construct was inserted into the *E.coli* expression vector PET28a(+) in between the EcoRI and BamHI restriction sites as shown in [Fig. 8](#). A 6-histidine tag was also included at both ends for the ease of purification of the recombinant vaccine through immune-chromatography. Thus, the length of the clone was 6.6 kbp.

RNA fold generated a secondary structure of the constructed vaccine sequence with a minimal free energy of -429.73 kcal/mol as illustrated in [Fig. 9](#).

### 3.16. Molecular docking of vaccine with TLR4 receptor

A docking study of vaccine protein with TLR4 was performed to estimate the binding affinity between the vaccine construct and TLR4. A total of 30 receptor-vaccine complexes were generated by ClusPro 2.0 and sorted by energy scores as tabulated in [Supplementary Table 22](#). Among these generated models, based on the energy scores model 2 showed the highest binding affinity (-1268. kcal/mol) and was finalized as the best-docked complex. Therefore, the best-docked complex was visualized using Pymol ([Fig. 10](#)).

### 3.17. Dynamics simulation of the vaccine-TLR4 complex

The stability and mobility of the protein-protein docked complex were evaluated by using the i-MODS tool, which calculates based on the dynamics of essential protein compared to their normal modes. The B-

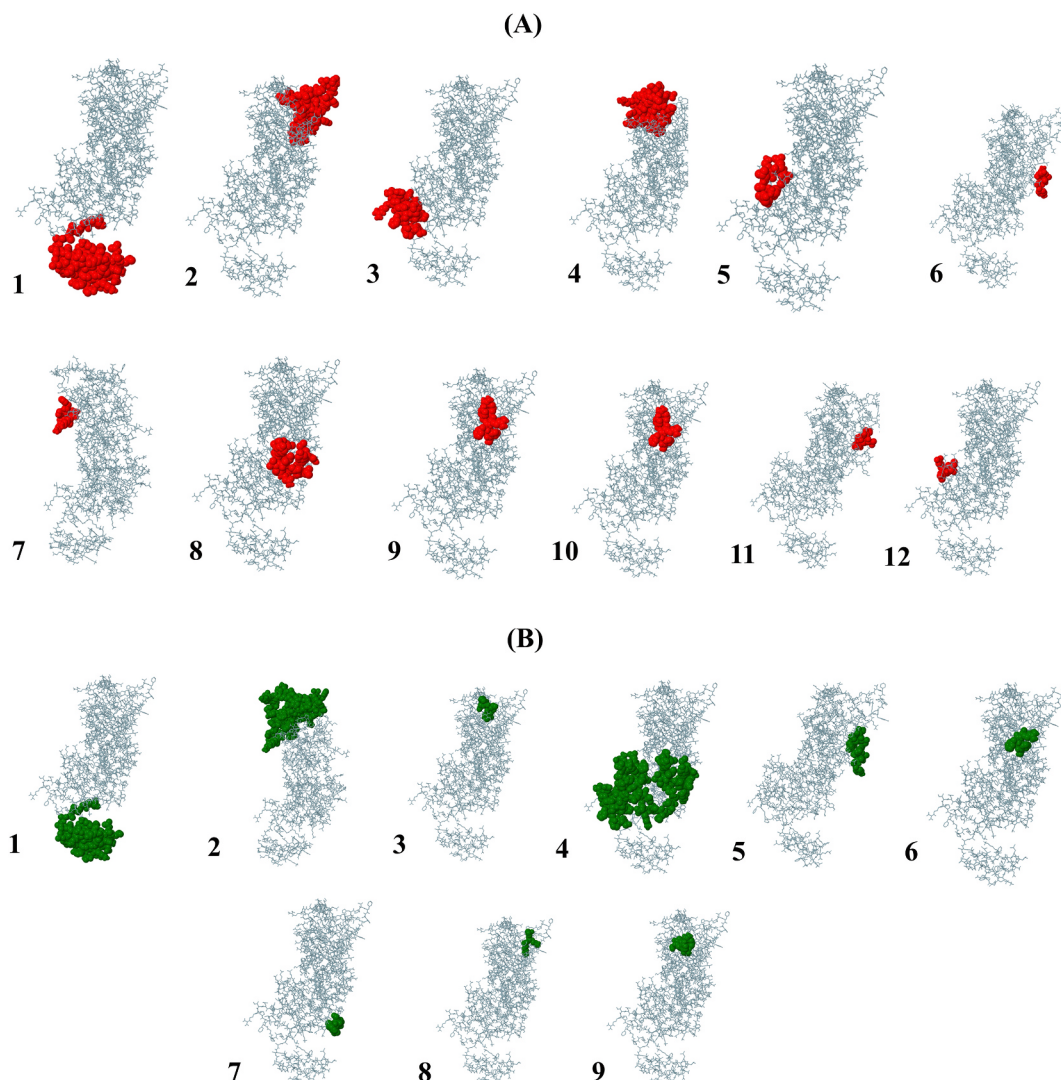


**Fig. 6.** Epitope mapping on the vaccine construct (A) red spheres showing linear B-cell epitopes containing 1.49 residues with 0.855, 2.34 residues with 0.771, 3.18 residues with 0.722, 4.48 residues with 0.716, 5.8 residues with 0.694, 6.5 residues with 0.642, 7.7 residues with 0.635, 8.18 residues with 0.608, 9.19 residues with 0.594, 10.7 residues with 0.579, 11.5 residues with 0.523 and 12.4 residues with 0.508 score. (B) green spheres indicate discontinuous B-cell epitopes containing 1.49 residues with 0.855, 2.78 residues with 0.738, 3.5 residues with 0.668, 4.67 residues with 0.629, 5.11 residues with 0.563, 6.5 residues with 0.562, 7.3 residues with 0.546, 8.3 residues with 0.539 and 9.5 residues with 0.528 score. (For interpretation of the references to color in this figure legend, the reader is referred to the Web version of this article.)

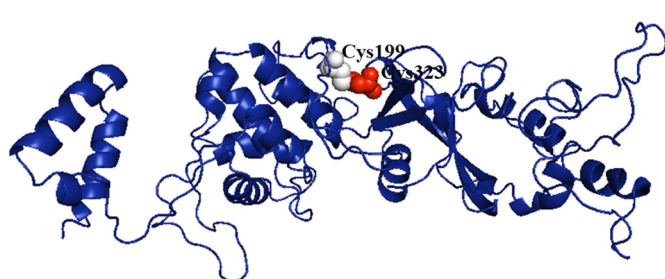


**Fig. 7.** Disulphide engineering of the final vaccine construct showing mutated residue pair in red (primary residue – A199) and blue (primary residue – G313) color. (For interpretation of the references to color in this figure legend, the reader is referred to the Web version of this article.)

factor values found from NMA represent the mobility of the docked complex which is proportional to the root mean square (RMS) value (Fig. 11a). The eigenvalue indicates the stiffness of a complex and the

eigenvalue found for our docked complex was  $2.656404e-05$  (Fig. 11b). The lower eigenvalue indicates easier deformation of a protein complex. Elastic network graph illustrates which pairs of atoms are linked by springs and each dot depicts one spring between a pair of atoms. The dots are colored according to their level of stiffness; darker gray dots mean stiffer springs (Fig. 11c). The covariance graph states the mobility types of a specific part of the molecule, where red, blue, and white colors indicate related, uncorrelated, and anti-related motions respectively (Fig. 11d). The main-chain deformability of a protein largely depends on the odds of individual residue being distorted, and residues having higher deformability values can be part of chain hinges illustrated by chain hinges (Fig. 11e). The variance graph shows the relative contribution of variance associated with each normal mode to the equilibrium motions where green and red bar indicates collective and individual variance respectively (Fig. 11f).

### 3.18. In silico immune response simulation

From the results generated by the C-ImmSim, it is obvious that

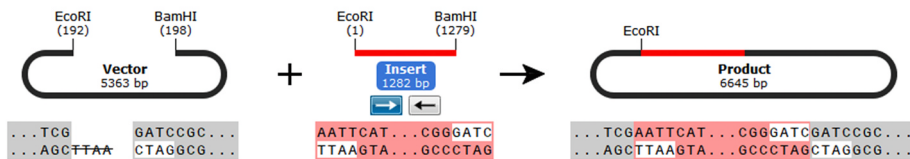
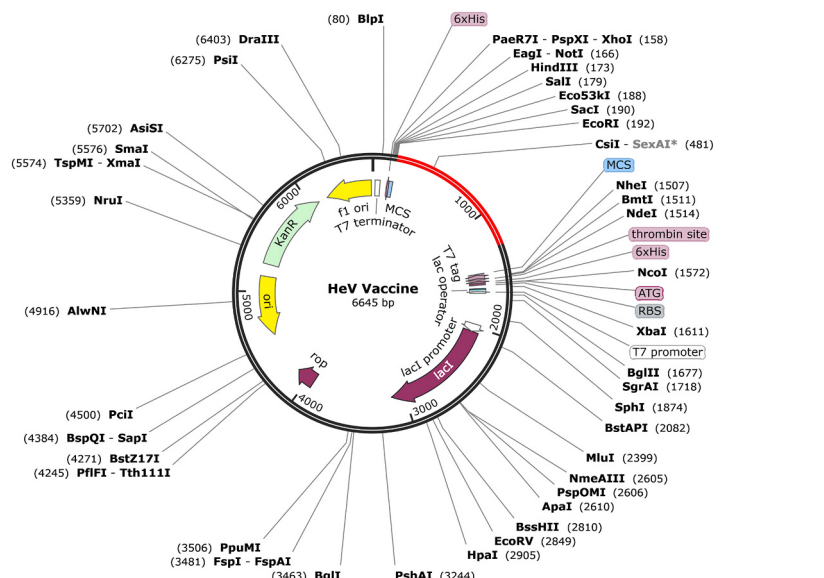


**Fig. 8.** In silico cloning of the optimized final vaccine construct into pET-28a (+) expression vector. Blue color shows the region of interest between EcoRI (192) and BamHI (1279) and black color represents the rest of the vector. (For interpretation of the references to color in this figure legend, the reader is referred to the Web version of this article.)

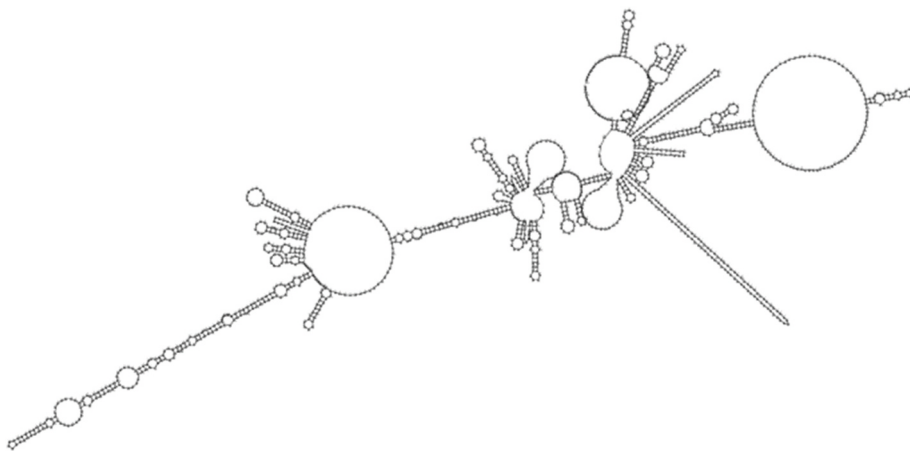


**Fig. 9.** Predicted mRNA secondary structure of the constructed vaccine construct.

primary immune response after vaccine administration is stimulated significantly with the gradual increase in the immunoglobulins level (i.e., IgM, IgG1, IgG2, IgG1 + IgG2, and IgG + IgM) during the secondary and tertiary immune response (Fig. 12a). The antigen level also decreased during the secondary and tertiary immune response. Besides, the elevated and sustained concentration of B-cell population (total, active and plasma B-cell) (Fig. 12b–c) and T-cell (helper T-cell, cytotoxic T-cell, regulatory T-cell) (Fig. 12d–j) were also evident indicating the potency of the designed vaccine. The concentration of Th1 was found increased after each shot (Fig. 12g). Furthermore, a higher level of dendritic and macrophage cells demonstrates the efficient antigen processing and presentation to the CD4<sup>+</sup> and CD8<sup>+</sup> cells by antigen-

presenting cells (APC) (Fig. 12k-l). Also, it is clear that the level of different kinds of cytokines also increased after exposure (Fig. 12m).

#### 4. Discussion

In recent times, vaccination has flourished as the most dynamic and promising approach to improve the immune mechanism that ultimately provides passive immunization against a specific pathogen to the host [63]. Development, improvement, and manufacturing of multiple forms of vaccine, like live or attenuated vaccines are expensive, tiresome, and generally takes a longer period to become commercially available [55, 63]. Besides, the attenuated vaccine provides mediocre passive

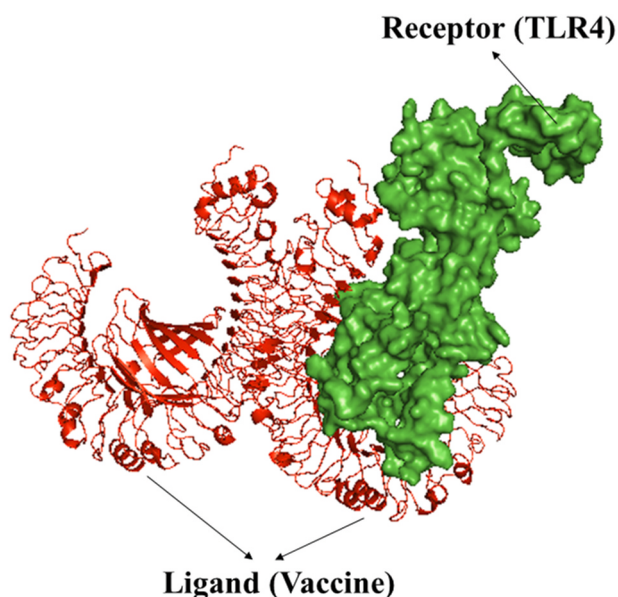


**Fig. 10.** Molecular docking simulation study of vaccine with TLR4 receptor showing TLR4 receptor as ribbon while vaccine as the surface view.

immunization and causes allergic reactions due to the excessive antigenic load [64]. They are overly simplistic for combating complex infectious agents [65]. Researchers have been devoted for a long time to develop cost-efficient, time-intensive, and safer vaccines for various infectious diseases. With the progression of multi-omics technology, the immunoinformatics approach becomes conceivable to decrease the burden of vaccine development by designing a newly potent peptide vaccine. The vaccine against *Neisseria meningitidis* was the first vaccine designed by the immunoinformatics approach and successfully manufactured later [66]. Besides, the capability to elicit immune responses focusing on conserved epitopes compared to the traditional vaccine [66] improves it as a better and safer therapeutic option. So far immunoinformatics approaches have been used to design multi-epitopes driven vaccines against Dengue virus, Ebola virus, Oropouche virus Hepatitis C virus, Human coronaviruses, Saint Louis encephalitis virus, Rhinovirus, etc. [66–68].

HeV is a rare but life-threatening zoonotic virus that has emerged at an alarming rate in recent times [1,7]. So, designing potential vaccines can be a blessing to fight against this lethal virus. In the current study, a potential vaccine has been proposed as an ideal candidate to prevent HeV infection. Three essential proteins related to the pathogenicity of the virus namely, glycoprotein, fusion protein, and nucleoprotein were selected based on their antigenicity score because the higher the antigenicity, the higher will be the immune response. Potential T and B-cell epitopes were predicted by using various databases and their suitability for use as a vaccine candidate were assessed. Finally, 7 CTL, 5 HTL, and 5 LBL epitopes were finalized considering their conservancy, interaction with the highest number of HLA alleles, highest antigenicity, immunogenicity, non-allergenicity, non-toxicity, cytokine inducing ability. In a previous study Parvege et al. [1], predicted two common epitopes LAEDDTNAQKT and LTDKIGTEI from G protein of NipV and HeV. In another study, Saha et al. [7], explored G, M and F protein of NipV and HeV to identify common epitopes to design a universal vaccine. Kamthania et al. [69], designed only T-cell epitopes by scrutinizing M, G, N, F, V, W and P proteins of HeV but the worldwide population coverage for predicted epitopes were not satisfactory. On the other hand, in our study the population coverage of the finalized T-cell (CTL and HTL) epitopes with their respective HLA alleles showed 95.3% global coverage. Furthermore, molecular docking simulation of HLA-A\*24:02 with CTL epitopes was performed where strong interaction of CTL epitopes with the HLA-A\*24:02 was found. Finally, to render a stable and potent

vaccine construct, AAY, and GPGPG linkers were placed in between the CTL, HTL, and LBL epitopes to ensure their immune response. To boost the immune reaction, *E. coli* (strain k12) derived 50s ribosomal L7/L12 which is a TLR4 agonist was used as an adjuvant and linked to the N-terminal of the vaccine construct with GPGPG linker while human beta-defensin adjuvant with GPGPG linker was added to the C-terminal.

The length of the constructed vaccine is 424 amino acids with a molecular weight of 44.90 kDa which is in the range of ideal molecular weight of chimeric vaccine. The pI value (8.49), instability index (30.91), GRAVY score (-0.004), and aliphatic index (85.73) of the designed vaccine respectively indicates its basic, stable, hydrophilic, and thermostable nature. Moreover, the vaccine's antigenicity (0.83) and immunogenicity value (4.86) and its non-allergenicity further proved its suitability as an effective vaccine. Solubility is one of the most fundamental and crucial criteria in vaccine production because higher solubility of the recombinant protein within the *E. coli* host results in easier isolation and purification. The constructed vaccine protein was found to be soluble upon overexpression in the *E. coli* host. In case of vaccine designing, short half-life of peptides is always a great concern and the designed chimeric vaccine successfully showed a satisfactory stability index that strongly recommended its potentiality as a HeV vaccine candidate.

Following the conformational analysis, 34.90% helix, 8.01% strands, and 57.07% random coils were predicted from the secondary structure of the designed protein. Ramachandra plot showed that the raw model had 70% amino acid in the favorable region while the refined model had 92.9% amino acid in the favorable region, 5.8% amino acid in the allowed region, and 0.8% amino acid in the disallowed region which elucidated that the designed model is satisfactory. Besides, RMSD (0.312), MolProbity (2.178), GDT-HA (0.9764), Poor rotamers (0.6) and Clash score (16.8) values indicated the excellent quality of the designed vaccine construct. Furthermore, the Z-score (-3.44) of the refined model depicted promising conformational quality of the vaccine construct. Therefore, all the validation results concluded that the tertiary structure of the vaccine construct is quite suitable for further analysis.

Increasing protein stability is conferred the utmost importance in various biomedical and therapeutic applications. To enhance the protein's thermostability and features, disulfide engineering was done and a pair of mutations introduced on the A199-G323 residue pair. *E. coli* cell culture system is widely used for the mass production of recombinant protein. Hence, optimization of codon concerning *E. coli* strain K12 was carried out for efficient expression in the host. From the obtained results, the GC content of 53.06% with the codon adaptability index (CAI) of 0.96 was optimized that ensures higher level of protein expression in *E. coli*.

Further, the molecular docking assay revealed that the designed vaccine binds at the receptor binding site of TLR4 with minimal binding energy (-1268 kcal/mol) indicating appropriate stronger binding affinity. Molecular dynamics simulation of the docked complex was done to evaluate the stability and mobility of the TLR4-vaccine complex in the biological environment. The eigenvalue (indicator of motion stiffness) for the TLR4-vaccine complex was found 2.656404e-05 which indicates the rigidity of the protein-protein complex and the complex requires higher energy to deform. The deformability graph further confirmed that the protein-protein complex is highly stable with a lower degree of each residue to be distorted as illustrated by chain hinges. Overall, molecular dynamics results showed that the designed vaccine is stable enough and there is a minimum chance of deformability at the molecular level.

Furthermore, the immune simulation results revealed that the vaccine construct generated an immune cascade against HeV antigen which mimics the natural immune reaction against viral pathogens. Upon administration of the vaccine, secondary and tertiary immune response was found higher than the primary response on the basis of significant amount of antibodies production and antigen clearance. An increase in

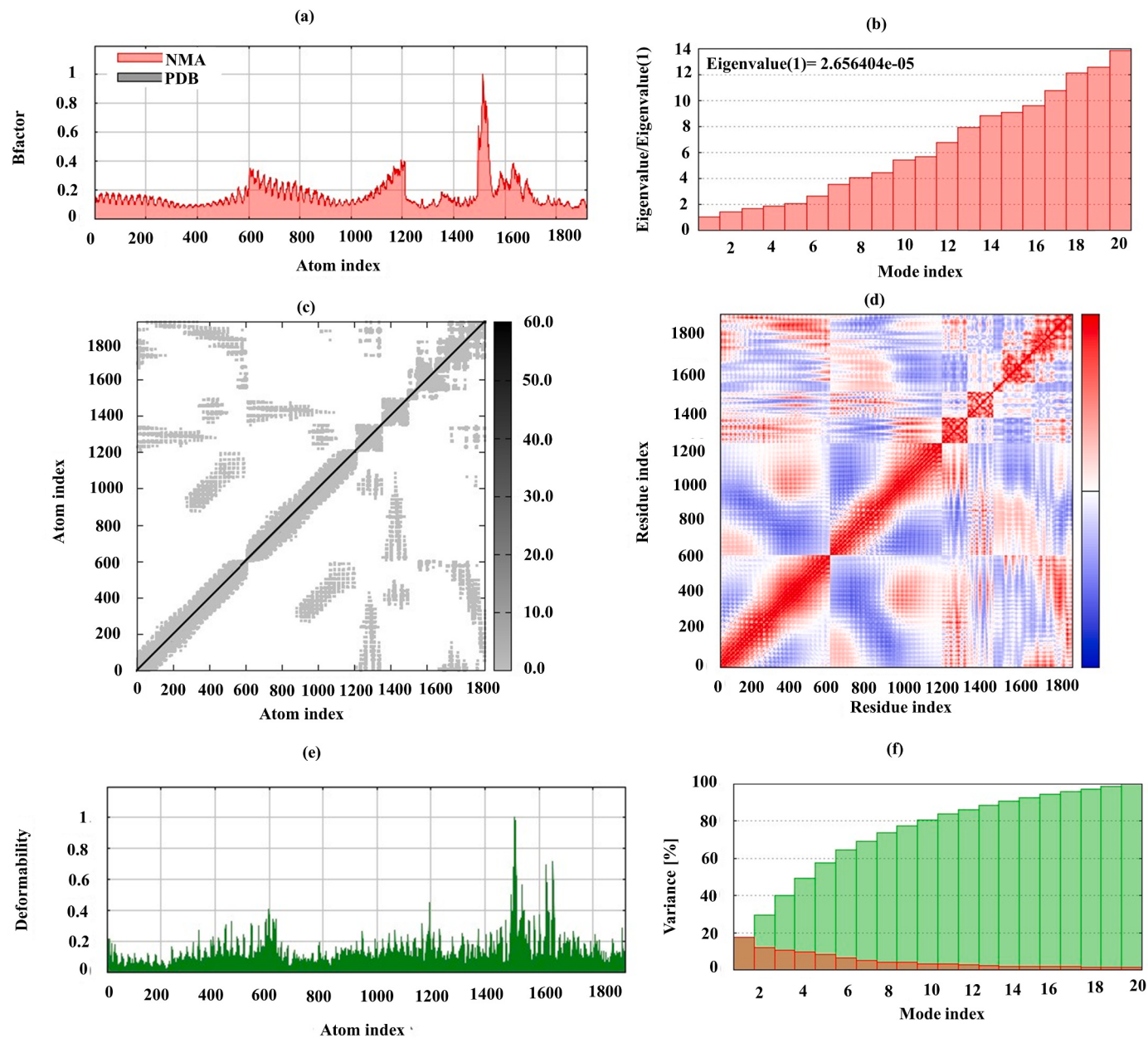


**Fig. 11.** Molecular dynamics simulation of the TLR4 – Vaccine complex showing (a) B factor (b) eigenvalue (c) elastic network (d) covariance matrix (e) deformability (f) variance.

the concentration of B-cells (memory B-cell, and plasma B-cell), and T-cells (cytotoxic and helper T-cell) confirmed that both cell-mediated and humoral immunity was stimulated by the vaccine. It is evident from the increased concentration of antigen processing cells like dendritic cells and macrophages that the vaccine construct is capable of inducing satisfactory antigen processing and presentation to the CD4<sup>+</sup> and CD8<sup>+</sup> cells (Fig. 12j–k). Besides, accumulation of cytokines indicates that there is a strong possibility to provoke broad-spectrum immunity against HeV invasions. However, further in vitro and in vivo validation is required to confirm the propositions.

To date, few attempts have been taken to suggest potential universal vaccines to be used as countermeasures against HeV [1,7,69], but success is yet to be noticed for the HeV vaccine production. Such universal vaccines for two closely related NipV and HeV cannot lead to successful immunization due to the subtle difference in pathogenesis, host-pathogen interaction, and immune response etc [70]. In this study, we have designed a potent multi-epitope-based HeV vaccine by utilizing

a systemic immunoinformatics approach. Despite the enormous potentiality of the immunoinformatics approach, it also might have some limitations to be proclaimed as a fully functional vaccine against HeV due to the absence of standard benchmark [65]. Besides, there is limited information on HeV pathogenesis and adaptive immune response against this virus [71,72]. Therefore, both in vivo and, in vitro experimental validation is required to assess the immunogenicity, efficacy, and safety of our newly designed vaccine.

## 5. Conclusion

HeV is an opportunistic, emerging zoonotic virus conferring a high fatality rate in humans. It has become a recurring threat to public health due to the lack of therapeutic agents for inhibiting its rapid affluence. We designed a novel and potent prophylactic multi-epitope-based vaccine against HeV which might be a possible therapeutic solution to prevent future outbreaks. We utilized an immunoinformatics approach

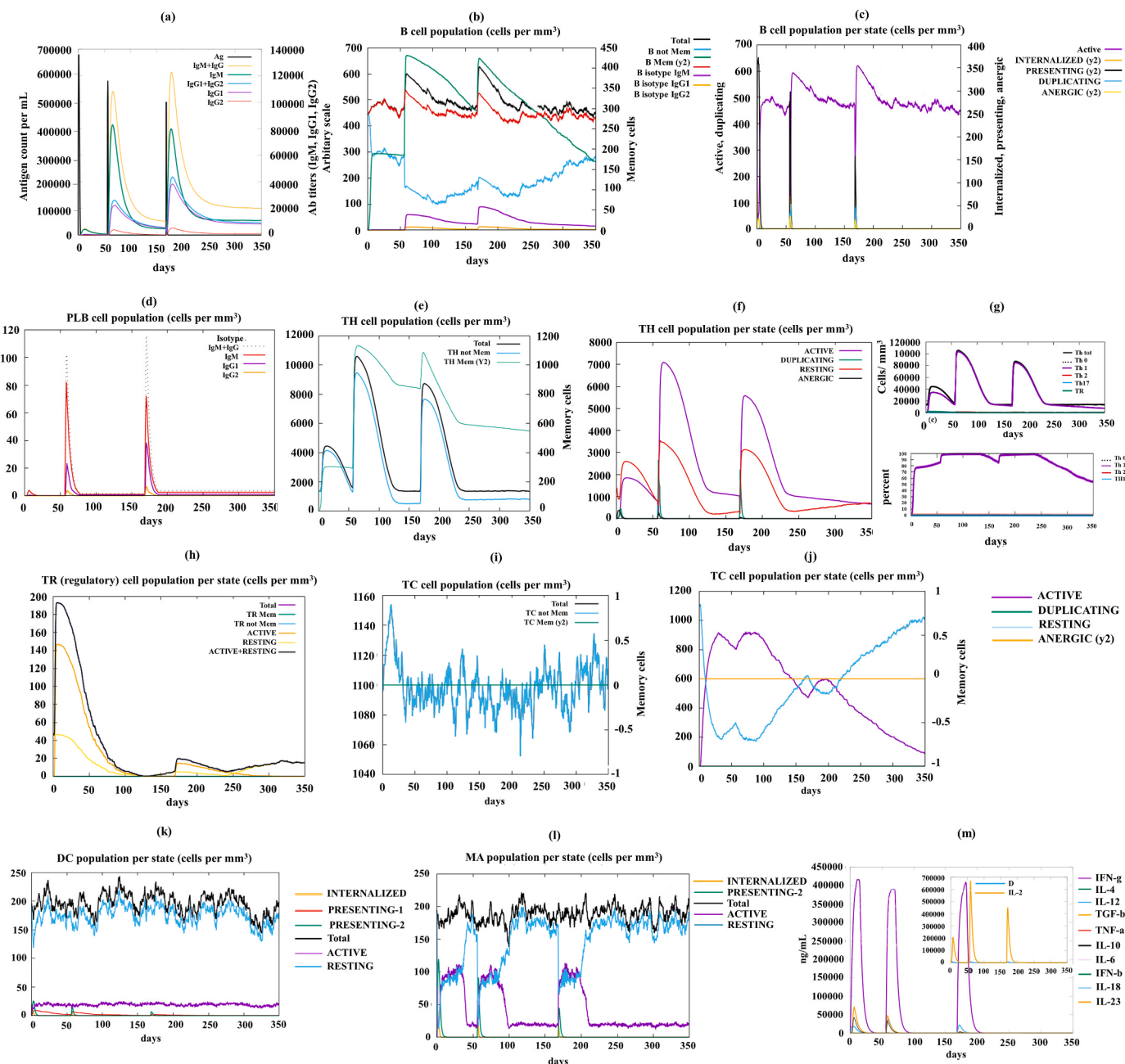


**Fig. 12.** In silico immune response simulation of the designed vaccine as antigen: (a) Antigen and immunoglobulins; (b) B-cell population; (c) B-cell population per state; (d) Plasma B-cell population; (e) Helper T-cell population; (f) Helper T-cell population per state; (g) Th1 cell population; (h) Regulatory T-cell population per state; (i) Cytotoxic T-cell population; (j) Cytotoxic T-cell population per state; (k) Dendritic cell population per state; (l) Macrophage population per state; and (m) Cytokines concentration with Simpson index (D) of the immune response.

followed by multiple bioinformatics tools along with molecular dynamics simulation and immune simulation to predict the efficacy of the designed construct as a novel multi-epitope vaccine. Data from our study revealed that our designed vaccine with further in vivo and in vitro validation can be used for an effective vaccine against HeV.

#### Credit authorship contribution statement

Mohammad Imran Hossan; Methodology, Formal analysis, Writing – Original Draft. Afrin Sultana Chowdhury: Conceptualization, Writing – Original Draft, Writing – Review & Editing, Supervision. Mohammad Uzzal Hossain: Validation, Writing – Review & Editing. Md. Arif Khan: Validation, Writing – Review, Tousif Bin Mahmood: Formal analysis,

Writing – Original Draft. Shagufta Mizan: Writing - Review & Editing.

#### Funding

This research did not receive any specific grant from funding agencies in the public, commercial, or not-for-profit sectors.

#### Declaration of competing interest

The authors declare that they have no known competing financial interests or personal relationships that could have appeared to influence the work reported in this paper.

## Acknowledgements

We thank Md. Mahbub Hasan from the University of Chittagong for his kind support.

## Appendix A. Supplementary data

Supplementary data to this article can be found online at <https://doi.org/10.1016/j imu.2021.100678>.

## References

- [1] Parvege MM, Rahman M, Nibir YM, Hossain MS. Two highly similar LAEDDTNAQKT and LTDKIGTEI epitopes in G glycoprotein may be useful for effective epitope based vaccine design against pathogenic Henipavirus. *Comput Biol Chem* 2016;61:270–80. <https://doi.org/10.1016/j.combiolchem.2016.03.001>.
- [2] Aljofan M. Hendra and nipah infection: emerging paramyxoviruses. *Virus Res* 2013;177:119–26. <https://doi.org/10.1016/j.virusres.2013.08.002>.
- [3] Field H, Crameri G, Kung NY-H, Wang L-F. Ecol. Aspec. Hendra Virus 2012;11–23. [https://doi.org/10.1007/82\\_2012\\_214](https://doi.org/10.1007/82_2012_214).
- [4] Marsh GA, Wang LF. Hendra and Nipah viruses: why are they so deadly? *Curr Opin Virol* 2012;2:242–7. <https://doi.org/10.1016/j.coviro.2012.03.006>.
- [5] Luby SP, Gurley ES. Epidemiology of Henipavirus Disease in Humans 2012:25–40. [https://doi.org/10.1007/82\\_2012\\_207](https://doi.org/10.1007/82_2012_207).
- [6] Playford EG, McCall B, Smith G, Slisko V, Allen G, Smith I, et al. Human Hendra virus encephalitis associated with equine outbreak, Australia. *Emerg Infect Dis* 2008;10(16):219–23. <https://doi.org/10.3201/eid1602.090552>.
- [7] Saha CK, Mahbub Hasan M, Saddam Hossain M, Asrafal Jahan M, Azad AK. In silico identification and characterization of common epitope-based peptide vaccine for Nipah and Hendra viruses. *Asian Pac J Trop Med* 2017;10:529–38. <https://doi.org/10.1016/j.apjtm.2017.06.016>.
- [8] Khusro A, Aarti C, Pliego AB, Cipriano-Salazar M. Hendra virus infection in horses: a review on emerging mystery paramyxovirus. *J Equine Vet Sci* 2020;103149. <https://doi.org/10.1016/j.jevs.2020.103149>.
- [9] Freiberg AN, Worthy MN, Lee B, Holbrook MR. Combined chloroquine and ribavirin treatment does not prevent death in a hamster model of Nipah and Hendra virus infection. *J Gen Virol* 2010;91:765–72. <https://doi.org/10.1099/vir.0.017269.0>.
- [10] Steffen DL, Xu K, Nikolov DB, Broder CC. Henipavirus mediated membrane fusion, virus entry and targeted therapeutics. *Viruses* 2012;4:280–309. <https://doi.org/10.3390/v4020280>.
- [11] Doytchinova IA, Flower DR. VaxiJen: a server for prediction of protective antigens, tumour antigens and subunit vaccines. *BMC Bioinf* 2007;8. <https://doi.org/10.1186/1471-2105-8-4>.
- [12] Krogh A, Larsson B, Von Heijne G, Sonnhammer ELL. Predicting transmembrane protein topology with a hidden Markov model: application to complete genomes. *J Mol Biol* 2001;305:567–80. <https://doi.org/10.1006/jmbi.2000.4315>.
- [13] Larsen MV, Lundsgaard C, Lamberth K, Buus S, Brunak S, Lund O, et al. An integrative approach to CTL epitope prediction: a combined algorithm integrating MHC class I binding, TAP transport efficiency, and proteasomal cleavage predictions. *Eur J Immunol* 2005;35:2295–303. <https://doi.org/10.1002/eji.200425811>.
- [14] Calis JJA, Maybeno M, Greenbaum JA, Weiskopf D, De Silva AD, Sette A, et al. Properties of MHC class I presented peptides that enhance immunogenicity. *PLoS Comput Biol* 2013;9. <https://doi.org/10.1371/journal.pcbi.1003266>.
- [15] Dimitrov I, Flower DR, Doytchinova I. AllerTOP - a server for in silico prediction of allergens. *BMC Bioinf* 2013;14. <https://doi.org/10.1186/1471-2105-14-S6-S4>.
- [16] Gupta S, Kapoor P, Chaudhary K, Gautam A, Kumar R, Raghava GPS. Silico approach for predicting toxicity of peptides and proteins. *PloS One* 2013;8. <https://doi.org/10.1371/journal.pone.0073957>.
- [17] Jurtz V, Paul S, Andreatta M, Marcatili P, Peters B, Nielsen M. NetMHCpan-4.0: improved peptide-MHC class I interaction predictions integrating eluted ligand and peptide binding affinity data. *J Immunol* 2017;199:3360–8. <https://doi.org/10.4049/jimmunol.1700893>.
- [18] Wang P, Sidney J, Dow C, Mothé B, Sette A, Peters B. A systematic assessment of MHC class II peptide binding predictions and evaluation of a consensus approach. *PLoS Comput Biol* 2008;4. <https://doi.org/10.1371/journal.pcbi.1000048>.
- [19] Dhanda SK, Gupta S, Vir P, Raghava GP. Prediction of IL4 inducing peptides. *Clin Dev Immunol* 2013;263952:2013. <https://doi.org/10.1155/2013/263952>.
- [20] Dhanda SK, Vir P, Raghava GP. Designing of interferon-gamma inducing MHC class-II binders. 2013.
- [21] Nagpal G, Usmani SS, Dhanda SK, Kaur H, Singh S, Sharma M, et al. Computer-aided designing of immunosuppressive peptides based on IL-10 inducing potential. *Sci Rep* 2017;7. <https://doi.org/10.1038/srep42851>.
- [22] Emini EA, Hughes J V, Perlow DS, Boger J. Induction of Hepatitis A Virus-Neutralizing Antibody by a Virus-Specific Synthetic Peptide Downloaded from. 1985.
- [23] Jespersen MC, Peters B, Nielsen M, Marcatili P. BepiPred-2.0: improving sequence-based B-cell epitope prediction using conformational epitopes. *Nucleic Acids Res* 2017;45:W24–9. <https://doi.org/10.1093/nar/gkx346>.
- [24] Bui HH, Sidney J, Li W, Fusseder N, Sette A. Development of an epitope conservancy analysis tool to facilitate the design of epitope-based diagnostics and vaccines. *BMC Bioinf* 2007;8. <https://doi.org/10.1186/1471-2105-8-361>.
- [25] Bui HH, Sidney J, Dinh K, Southwood S, Newman MJ, Sette A. Predicting population coverage of T-cell epitope-based diagnostics and vaccines. *BMC Bioinf* 2006;7. <https://doi.org/10.1186/1471-2105-7-153>.
- [26] Lamiable A, Thévenet P, Rey J, Vavrusa M, Derreumaux P, Tufféry P. PEP-FOLD3: faster de novo structure prediction for linear peptides in solution and in complex. *Nucleic Acids Res* 2016;44:W449–54. <https://doi.org/10.1093/nar/gkw329>.
- [27] Berman HM, Westbrook J, Feng Z, Gilliland G, Bhat TN, Weissig H, et al. The Protein Data Bank 2000;28.
- [28] Morris GM, Ruth H, Lindstrom W, Sanner MF, Belew RK, Goodsell DS, et al. Software news and updates AutoDock4 and AutoDockTools4: automated docking with selective receptor flexibility. *J Comput Chem* 2009;30:2785–91. <https://doi.org/10.1002/jcc.21256>.
- [29] Trott O, Olson AJ. AutoDock Vina: improving the speed and accuracy of docking with a new scoring function, efficient optimization, multithreading. *J Comput Chem* 2009. <https://doi.org/10.1002/jcc.21334>. NA-NA.
- [30] Delano WL. PyMOL: An Open-Source Molecular Graphics Tool. n.d.
- [31] Pandey RK, Bhatt TK, Prajapati VK. Novel immunoinformatics approaches to design multi-epitope subunit vaccine for malaria by investigating Anopheles salivary protein. *Sci Rep* 2018;8. <https://doi.org/10.1038/s41598-018-19456-1>.
- [32] Coffman RL, Sher A, Seder RA. Vaccine adjuvants: putting innate immunity to work. *Immunity* 2010;33:492–503. <https://doi.org/10.1016/j.imuni.2010.10.002>.
- [33] Gu Y, Sun X, Li B, Huang J, Zhan B, Zhu X. Vaccination with a paramyosin-based multi-epitope vaccine elicits significant protective immunity against *Trichinella spiralis* infection in mice. *Front Microbiol* 2017;8. <https://doi.org/10.3389/fmicb.2017.01475>.
- [34] Magnan CN, Zeller M, Kayala MA, Vigil A, Randall A, Felgner PL, et al. High-throughput prediction of protein antigenicity using protein microarray data. *Bioinformatics* 2010;26:2936–43. <https://doi.org/10.1093/bioinformatics/btq551>.
- [35] Gasteiger E, Hoogland C, Gattiker A, Duvaud S, Wilkins MR, Appel RD, et al. Protein Analysis Tools on the ExPASy Server 571 571 from: The Proteomics Protocols Handbook Protein Identification and Analysis Tools on the ExPASy Server. n.d.
- [36] Magnan CN, Randall A, Baldi P. SOLpro: accurate sequence-based prediction of protein solubility. *Bioinformatics* 2009;25:2200–7. <https://doi.org/10.1093/bioinformatics/btp386>.
- [37] Hebditch M, Carballo-Amador MA, Charonis S, Curtis R, Warwicker J. Protein-Sol: a web tool for predicting protein solubility from sequence. *Bioinformatics* 2017;33: 3098–100. <https://doi.org/10.1093/bioinformatics/btx345>.
- [38] McGuffin LJ, Bryson K, Jones DT. The PSIPRED protein structure prediction server 2000;16.
- [39] Roy A, Kucukural A, Zhang Y. I-TASSER: a unified platform for automated protein structure and function prediction. *Nat Protoc* 2010;5:725–38. <https://doi.org/10.1038/nprot.2010.5>.
- [40] Bhattacharya D, Nowotny J, Cao R, Cheng J. 3Drefine: an interactive web server for efficient protein structure refinement. *Nucleic Acids Res* 2016;44:W406–9. <https://doi.org/10.1093/nar/gkw336>.
- [41] Heo I, Park H, Seok C. GalaxyRefine: protein structure refinement driven by side-chain repacking. *Nucleic Acids Res* 2013;41. <https://doi.org/10.1093/nar/gkt458>.
- [42] Wiederstein M, Sippel MJ. ProSA-web: interactive web service for the recognition of errors in three-dimensional structures of proteins. *Nucleic Acids Res* 2007;35: 3098–100. <https://doi.org/10.1093/nar/gkm290>.
- [43] Waterhouse A, Bertoni M, Bienert S, Studer G, Tauriello G, Gumienny R, et al. SWISS-MODEL: homology modelling of protein structures and complexes. *Nucleic Acids Res* 2018;46:W296–303. <https://doi.org/10.1093/nar/gky427>.
- [44] Ponomarenko J, Bui HH, Li W, Fusseder N, Bourne PE, Sette A, et al. ElliPro: a new structure-based tool for the prediction of antibody epitopes. *BMC Bioinf* 2008;9. <https://doi.org/10.1186/1471-2105-9-514>.
- [45] Craig D, Bmc D, Craig DB, Dombrowski AA. Disulfide by Design 2.0: a web-based tool for disulfide engineering in proteins 2013;14.
- [46] Grote A, Hiller K, Scheer M, Münnich R, Nörtemann B, Hempel DC, et al. JCat: a novel tool to adapt codon usage of a target gene to its potential expression host. *Nucleic Acids Res* 2005;33. <https://doi.org/10.1093/nar/gki376>.
- [47] Mathews DH, Sabina J, Zuker M, Turner DH. Expanded sequence dependence of thermodynamic parameters improves prediction of RNA secondary structure. *J Mol Biol* 1999;288:911–40. <https://doi.org/10.1006/jmbi.1999.2700>.
- [48] Mathews DH, Turner DH, Watson RM. RNA secondary structure prediction. *Curr Protoc Nucleic Acid Chem* 2016;2016:11.2.1–11.2.19. <https://doi.org/10.1002/cnc.19>.
- [49] Gruber AR, Lorenz R, Bernhart SH, Neuböck R, Hofacker IL. The Vienna RNA website. *Nucleic Acids Res* 2008;36. <https://doi.org/10.1093/nar/gkn188>.
- [50] Kozakov D, Hall DR, Xia B, Porter KA, Padhorny D, Yueh C, et al. The ClusPro web server for protein-protein docking. *Nat Protoc* 2017;12:255–78. <https://doi.org/10.1038/nprot.2016.169>.
- [51] López-Blanco JR, Aliaga JI, Quintana-Ortí ES, Chacón P. IMODS: internal coordinates normal mode analysis server. *Nucleic Acids Res* 2014;42. <https://doi.org/10.1093/nar/gku339>.
- [52] Rapin N, Lund O, Bernaschi M, Castiglione F. Computational immunology meets bioinformatics: the use of prediction tools for molecular binding in the simulation of the immune system. *PloS One* 2010;5. <https://doi.org/10.1371/journal.pone.0009862>.

- [54] Castiglione F, Mantile F, De Berardinis P, Prisco A. How the interval between prime and boost injection affects the immune response in a computational model of the immune system. *Comput Math Methods Med* 2012;2012. <https://doi.org/10.1155/2012/842329>.
- [55] Nain Z, Abdullah F, Rahman MM, Karim MM, Khan MSA, Bin Sayed S, et al. Proteome-wide screening for designing a multi-epitope vaccine against emerging pathogen *Elizabethkingia anophelis* using immunoinformatic approaches. *J Biomol Struct Dyn* 2019. <https://doi.org/10.1080/07391102.2019.1692072>.
- [56] Chaudhri G, Quah BJ, Wang Y, Tan AHY, Zhou J, Karupiah G, et al. T cell receptor sharing by cytotoxic T lymphocytes facilitates efficient virus control. *Proc Natl Acad Sci U S A* 2009;106:14984–9. <https://doi.org/10.1073/pnas.0906554106>.
- [57] Nielsen M, Lundsgaard C, Lund O. Prediction of MHC class II binding affinity using SMM-align, a novel stabilization matrix alignment method. *BMC Bioinf* 2007;8:1–12. <https://doi.org/10.1186/1471-2105-8-238>.
- [58] Dittmer U, Peterson KE, Messer R, Strommes IM, Race B, Hasenkrug KJ. Role of interleukin-4 (IL-4), IL-12, and gamma interferon in primary and vaccine-primed immune responses to friend retrovirus infection. *J Virol* 2001;75:654–60. <https://doi.org/10.1128/jvi.75.2.654-660.2001>.
- [59] Rojas JM, Avia M, Martín V, Sevilla N. IL-10: a multifunctional cytokine in viral infections. *J Immunol Res* 2017;2017. <https://doi.org/10.1155/2017/6104054>.
- [60] Cooper MD. The early history of B cells. *Nat Rev Immunol* 2015;15:191–7. <https://doi.org/10.1038/nri3801>.
- [61] Adhikari UK, Rahman MM. Overlapping CD8 + and CD4 + T-cell epitopes identification for the progression of epitope-based peptide vaccine from nucleocapsid and glycoprotein of emerging Rift Valley fever virus using immunoinformatics approach. *Infect Genet Evol* 2017;56:75–91. <https://doi.org/10.1016/j.meegid.2017.10.022>.
- [62] Lund FE. Cytokine-producing B lymphocytes-key regulators of immunity. n.d.
- [63] Nezafat N, Karimi Z, Eslami M, Mohkam M, Zandian S, Ghasemi Y. Designing an efficient multi-epitope peptide vaccine against *Vibrio cholerae* via combined immunoinformatics and protein interaction based approaches. *Comput Biol Chem* 2016;62:82–95. <https://doi.org/10.1016/j.compbiochem.2016.04.006>.
- [64] Bin Sayed S, Nain Z, Khan MSA, Abdulla F, Tasmin R, Adhikari UK. Exploring lassa virus proteome to design a multi-epitope vaccine through immunoinformatics and immune simulation analyses. *Int J Pept Res Ther* 2020. <https://doi.org/10.1007/s10989-019-10003-8>.
- [65] Khan F, Srivastava V, Kumar A. Computational identification and characterization of potential T-cell epitope for the utility of vaccine design against enterotoxigenic *Escherichia coli*. *Int J Pept Res Ther* 2019;25:289–302. <https://doi.org/10.1007/s10989-018-9671-3>.
- [66] Adu-Bobie J, Capecchi B, Serruto D, Rappuoli R, Pizza M. Two years into reverse vaccinology 2003;21.
- [67] Kalyanaraman N. In silico prediction of potential vaccine candidates on capsid protein of human bocavirus 1. *Mol Immunol* 2018;93:193–205. <https://doi.org/10.1016/j.molimm.2017.11.024>.
- [68] Hasan MA, Khan MA, Datta A, Mazumder MHH, Hossain MU. A comprehensive immunoinformatics and target site study revealed the corner-stone toward Chikungunya virus treatment. *Mol Immunol* 2015;65:189–204. <https://doi.org/10.1016/j.molimm.2014.12.013>.
- [69] Kamthania M, Srivastava S, Desai M, Jain A, Shrivastav A, Sharma DK. Immunoinformatics approach to design T-cell epitope-based vaccine against Hendra virus. *Int J Pept Res Ther* 2019;25:1627–37. <https://doi.org/10.1007/s10989-018-09805-z>.
- [70] Weingartl H. Hendra and Nipah viruses: pathogenesis, animal models and recent breakthroughs in vaccination. *Vaccine Dev Ther* 2015;59. <https://doi.org/10.2147/vdt.s86482>.
- [71] Mathieu C, Horvat B. Henipavirus pathogenesis and antiviral approaches. *Expert Rev Anti Infect Ther* 2015;13:343–54. <https://doi.org/10.1586/14787210.2015.1001838>.
- [72] Escaffre O, Borisevich V, Rockx B. Pathogenesis of Hendra and Nipah virus infection in humans. *J Infect Dev Ctries* 2013;7:308–11. <https://doi.org/10.3855/jidc.3648>.